# Acoustic emission monitoring of degradation of cross ply laminates

**D. G. Aggelis,[a] N. M. Barkoula, T. E. Matikas, and A. S. Paipetis**
*Department of Materials Science and Engineering, University of Ioannina, Ioannina 45110, Greece*
*daggelis@cc.uoi.gr, nbarkoul@cc.uoi.gr, matikas@cc.uoi.gr, paipetis@cc.uoi.gr*

**Abstract:** The scope of this study is to relate the acoustic activity of damage in composites to the failure mechanisms associated with these materials. Cross ply fiber reinforced composites were subjected to tensile loading with recording of their acoustic activity. Acoustic emission (AE) parameters were employed to monitor the transition of the damage mechanism from transverse cracking (mode I) to delamination (mode II). Wave propagation measurements in between loading steps revealed an increase in the relative amplitude of the propagated wave, which was attributed to the development of delamination that confined the wave to the top longitudinal plies of the composite.



**PACS numbers:** 43.40.Le, 43.35.Zc [JM]
**Date Received:** November 10, 2009 **Date Accepted:** April 12, 2010

## 1. Introduction

Multidirectional composites are prone to various forms of damage when they are subjected to mechanical loading. This damage is different in nature to damage observed in isotropic materials in that fibrous composites inherently possess macroscopic anisotropy which, at the lamina scale is translated in a steep property change. The typical failure behavior of cross-ply laminates starts by the premature failure of the plies containing fibers oriented transversely to the loading axis, which is known as transverse or interlaminar cracking. This failure creates the shear discontinuity at the lamina scale and the respective stress magnification which triggers all other damage mechanisms.[1] Numerous studies have been performed to study the triggering of the aforementioned mechanisms, their succession and finally their accumulation that leads to the global failure of the composite.[2]

In general, transverse cracking creates a stress concentration at the neighboring 0° plies. Depending on the interlaminar strength, the crack may be deflected to the 0°/90° interlaminar surface causing delamination or proceed in the 0° ply causing longitudinal fiber failure. Transverse cracking is typical of a mode I crack or a tensile crack, whereas delamination is typical of a mode II crack or a shear crack.[3] As is well known, there is a trade off between low interlaminar strength that favors a damage tolerant structure and high interlaminar strength that maximizes the reinforcing ability of all ply orientations. From the above postulations, it is obvious that a good knowledge of the initiation and propagation of the distinct damage mechanisms will provide an insight into the strengthening mechanisms and aid the designer toward the optimization of the interlaminar/interfacial properties.

The acoustic emission (AE) technique has been employed in numerous applications for damage characterization on composite materials.[4–7] Suitable sensors are placed on the surface in order to record the transient waves (hits) generated by damage initiation and propagation inside the material. Moreover, AE has been successfully applied in cross ply composites in order to separate the acoustic activity of various damage modes in a cross ply composite.[4]

Further study of the transient waveforms may provide in depth insight of the fracture process. The source of the AE activity is closely connected to the mode of fracture.[8] If the failure sequence is determined, it is possible to tailor the properties of the constituent phases

[a]Author to whom correspondence should be addressed.

 

and their interface using proper design or materials so as to optimize the resistance against the specific failure mode. As has already been mentioned, this optimization does not necessarily coincide with maximum strength.

In general, the nucleation of shear cracks generally follows the propagation of tensile cracks. In case of cross ply laminates, transverse cracking (mode I) of the 90° plies is a prerequisite for the creation of the shear discontinuity that will trigger further failure mechanisms and by definition precedes interlaminar shear or delaminations (mode II). Within the scope of this study is to evaluate qualitatively and quantitatively the signature of mode I and mode II failure in the acoustic activity of the loaded composite.

In the engineering field the shape of the AE waveforms is reported to be characteristic of the fracture mode. Shear events are characterized by longer rise time (RT) (time delay between the first threshold crossing and the maximum peak) and usually lower peak amplitude ($A$) (voltage of the largest cycle) than tensile events.[9,10] This is examined by the RA value which is defined as the ratio of the RT (expressed in $\mu$s) to the waveform amplitude, $A$ (expressed in V).[11] It has been shown that lower RA values, indicate tensile nature of fracture events.[9,10]

## 2. Experimental details

The cross-ply laminates were fabricated by hand layup with a sequence $[0^{\circ}_{4}/90^{\circ}_{4}]_{s}$, resulting in a number of 16 plies with total specimen thickness of 2 mm. The UD 220 $\mathrm{g/m^2}$ (Aero) unidirectional glass fiber fabric was impregnated using the HT2 epoxy resin/hardener matrix system (mixing ratio 100:48) manufactured by R&G Faserverbundwerkstoffe GmbH Composite Technology. A $250\times 250\ \mathrm{mm^2}$ laminate was manufactured and was allowed to cure for 24 h at room temperature. Tensile specimens were subsequently cut according to the ASTM D3039 standard, at a width of 20 mm each.

The tensile specimens were loaded in load controlled tension, in a step loading mode. The loading spectrum was a saw-tooth spectrum formed from a sequence of triangular loading/unloading steps. A rate 5 kN/min was employed for both loading and unloading. The maximum load was incremented by 4 kN at each consecutive step. The step loading continued until the tensile failure of the specimen. All tensile tests were performed using an Instron Universal Testing Machine equipped with hydraulic gripping system, under load control, at controlled environmental conditions of 25 °C and 70% relative humidity.

For the purpose of the AE monitoring, two wide band AE sensors (Pico, Physical Acoustics Corp., PAC) were attached on the same side of the specimen. Electron wax was applied between the sensor and the specimen to enhance acoustic coupling, while it offered the necessary support to the sensors during the experiment. The specific sensors were chosen over other AE transducers mainly due to their spectral response. They are sensitive to frequencies from 100 kHz up to approximately 800 kHz, with maximum sensitivity at 500 kHz. Therefore, they can capture a wide range of different sources. The distance between the two receivers was 70 mm. For the purpose of wave propagation measurements another transducer (PAC, R6) was attached to the specimen at a distance of 20 mm from the first receiver. The sensor was connected to a pulse generator which introduced successive signals of 10 cycles of 100, 200, 300, 400 and 500 kHz during the intermittence between the load steps. By comparing the transient response of the two receivers, wave transmission measurements were performed on the 70 mm span between them.

The pre-amplifier gain was set to 40 dB. After performing a pilot test, the threshold was also set to 40 dB in order to avoid the possibility of electronic/environmental noise. The signals were recorded in a two-channel monitoring board PCI-2, PAC. AE hits were recorded with a sampling rate of 5 MHz. The AE activity increased progressively for each successive load step from a few hundred hits at the first step to more than 10 000 for the last.

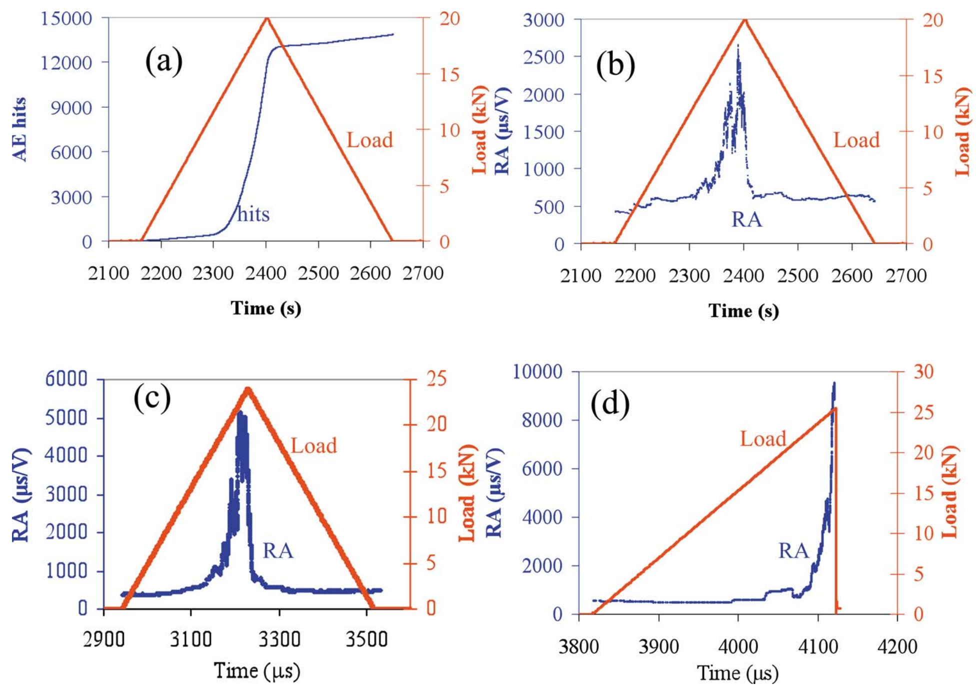


Fig. 1. (Color online) (a) Load history and AE cumulative hits for step 5, load history and RA value for step 5 (b), step 6 (c), step 7(d).

### 3. AE results

It is essential to present the AE results along with the mechanical data for reference. The most indicative trends concern the RA value shift to higher levels as the load increases. The discussion is focused on later loading steps since the initial loading steps exhibited little AE activity. Some typical cases are presented below.

Figure 1(a) depicts the load history of the fifth step corresponding roughly to the time span 2150 s to 2650 s of a single experiment. The load increases linearly with time until the maximum programed value of 20 kN and afterwards it decreases linearly with the opposite rate. On the same figure the AE cumulative hits are depicted. The first hits are recorded shortly after the application of load. However, significant increase in the hit rate is exhibited after the load passed approximately 12 kN (near 2300 s). Then the hit rate remains high and approximately constant until the maximum load. After the maximum load is reached the hit rate decreases but does not drop to zero. In Fig. 1(b) the load history of the same specimen at the same step along with the transition of the RA value are depicted as a function of time. Until about half the maximum load, the RA exhibits a constant value of approximately 500 $\mu$s/V. As the load rises further, the RA value clearly increases despite some fluctuations. After the maximum load is reached, the RA drops immediately to the initial value of 500 $\mu$s/V. It should be mentioned that the plotted RA value represents a moving average of the last 500 hits. As explained in the Introduction, the RA shift to higher values indicates that more shear events occur in the specimen. This is consistent with the succession of the failure mechanisms that are expected for the tested materials, since transverse i.e., mode I cracking initially takes place in order to trigger delaminations i.e., mode II cracking which dominate later loading steps as transverse cracking asymptotically reaches saturation. This trend is also consistent for the following loading steps until the failure of the specimen [Figs. 1(c) and 1(d)].

During step 6 [Fig. 1(c)], the RA increases to higher levels of almost 6000 $\mu$s/V, while during the unloading stage it drops again to less than 1000 $\mu$s/V. As for the final stage [step

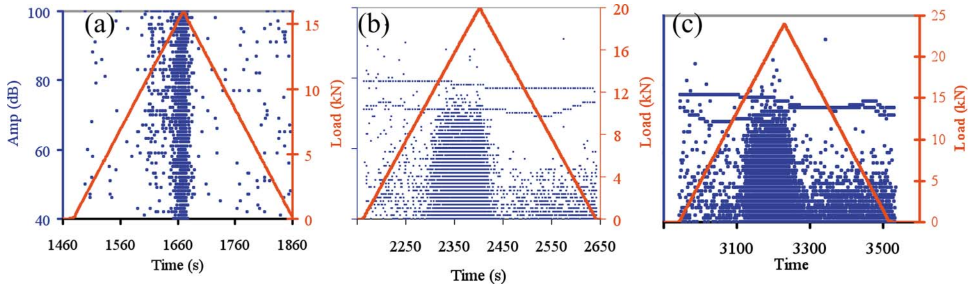


Fig. 2. (Color online) Load and AE amplitude for steps 4 (a), 5 (b) and 6 (c).

7 for the specific specimen which failed at 25.5 kN, see Fig. 1(d)] the moving average of RA reaches almost 10 000 $\mu s/V$ before the experiment is terminated due to the failure of the specimen. The increase of the RA value throughout each step suggests that shear failure or delamination is becoming more and more prominent as a failure mode. Additionally, each successive load step results in higher maximum RA values, which indicates that delaminations become the dominant damage mode at late loading steps, when transverse cracking is near or has reached saturation. Although failure is associated with the failure of the longitudinal plies, the moment of failure the RA exhibits its highest value, suggesting that shear cracking is the dominant mechanism prior to catastrophic failure. This behavior is consistent for all specimens studied and suggests that the RA value can be potentially used to study the tensile to shear mode conversion in composite systems in order to tailor the interlaminar properties of the material for maximum performance.

When a symmetric loading and unloading pattern is applied, the acoustic emission during the two distinct phases can be quantified. It is generally accepted that when the material is undamaged, the activity during unloading is negligible compared to that of loading. However, when damage has been accumulated a significant number of AE events are recorded even at the unloading stage. This behavior is quantified by the "calm ratio" (CR) which is the ratio of the AE hits during unloading to the hits of the whole cycle.[12] In the engineering field it is accepted that values below 0.05 indicate healthy state while values higher than 0.1 are connected to extended damage. In Fig. 2 three successive load steps of a specimen are depicted along with the corresponding AE activity. The symbols stand for the amplitude of each hit. At Fig. 2(a) which concerns load step 4 out of 7, a small number of hits is recorded after the maximum load, leading to a CR of 0.046. At the next step [Fig. 2(b)], the AE hits of unloading clearly increase resulting in a CR of 0.144. At step 6 [Fig. 2(c)], where the load reached 24 kN, and which was the last before the final step, the CR increased to 0.169. Based solely on this value it would be easy to predict that the structural health of the component had been severely compromised. Actually the specimen failed on the next step at the load of 25.5 kN. It is worth to mention that for all the specimens of this study the CR before the final stage was between 0.12 and 0.17 and it was the maximum value exhibited for each specimen.

The above mentioned parameters show that certain AE indices can be used to characterize the damage process of laminated composite materials.

## 4. Wave propagation measurements

As mentioned earlier, except the two AE sensors, another transducer acting as pulser was attached to the specimen in order to conduct wave velocity and transmission measurements during the intervals between successive loading steps. Tone bursts of different frequencies were fed to the transducer and the response of the sensors was recorded. In order to increase the signal to noise ratio, 100 signals were recorded and stacked. Due to attenuation mechanisms which include geometric spreading, and damping the amplitude captured by the second receiver is lower than the first. Additionally, due to scattering on damage-induced cracks during the experiment, the ratio of amplitudes of the second over the first is expected to change depending on the load step. It would be reasonable to expect that as damage in the form of micro-cracks evolves, the

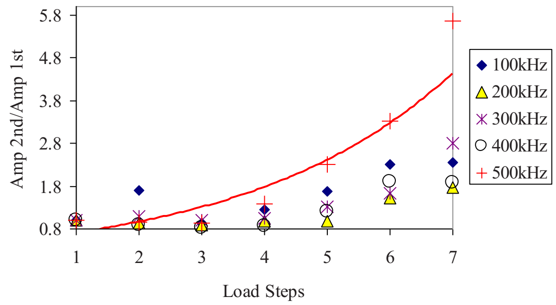


Fig. 3. (Color online) Transmission for different frequencies and loading step.

amplitude of the second receiver would be decreasing. However, in the present case, there is another strong damage mechanism due to delaminations. As delaminations are accumulated the different layers become separated. The pulser introduces the signal on the top 0° layer. Due to interlaminar failure, the signal propagation on the underlying 90° layers is partially restricted. Therefore, the energy is not spread but concentrated on the top layer. The behavior of the ratio of amplitudes of the second over the first receiver is depicted in Fig. 3. As seen, the amplitude is increased for all the frequencies tested. After the first two steps the amplitude ratio is monotonically increasing until failure, more likely being governed by the progressive delaminations which isolate the wave to the top layer. Before the final step, the transmission is approximately double than the initial stage. Thus, this increase in transmitted amplitude can be directly associated to interlaminar failure or the extend of delamination that the specimen can sustain before failure. As should be noted, the longitudinal plies (0°, parallel to the load direction) are an order of magnitude stiffer than the transverse plies in the wave propagation direction, which could also account for the increasing tendency of the pulse velocities which was exhibited, though not as consistently as amplitude.

It is mentioned that more elaborate study of the whole collected waveforms will enable the discrimination of individual plate wave modes and potentially enhance the characterization capacity since the type of damage may influence in a different way the individual modes.

## 5. Conclusions

In this study the mechanical and acoustic emission behavior of GFRP composite laminates is examined under triangular step loading. AE parameters like the RA value and calm ratio are found to be sensitive to the failure mode and accumulation, since they gradually shift as the dominant failure mode changes from transverse cracking to delamination. Therefore, they can act as damage indices associated to the damage conversion in cross ply composites with increasing load. Wave transmission measurements are found to be sensitive to delaminations due to the partial restriction of the wave energy on the top layer. This has an adverse effect on the amplitude of the transmitted signal compared to the effect of damage in the wave propagation of macroscopically homogeneous and isotropic materials.

## References and links


[1]D. G. Katerelos, L. N. McCartney, and C. Galiotis, "Local strain re-distribution and stiffness degradation in cross-ply polymer composites under tension," Acta Mater. **53**, 3335–3343 (2005).

[2]J. Nairn and S. Hu, "Matrix microcracking," in *Damage Mechanics of Composite Materials*, Composite Materials Series Vol. **9**, edited by R. B. Pipes and R. Talreja (Elsevier, Amsterdam, 1994).

[3]D. Callister, Jr., *Materials Science and Engineering, An Introduction* (Wiley, New York, 2000).

[4]D. G. Katerelos, A. S. Paipetis, T. Loutas, G. Sotiriadis, V. Kostopoulos, and S. L. Orgin, "In situ damage monitoring of cross-ply laminates using acoustic emission," Plast. Rubber Compos. **38**, 229–234 (2009).

[5]W. H. Prosser, "The propagation characteristics of the plate modes of acoustic emission waves in thin aluminum plates and thin graphite/epoxy composite plates and tubes," J. Acoust. Soc. Am. **92**, 3441–3442 (1992).

[6]N. Vasudevan and A. W. Shaker, "Acoustic emission from a nucleating point fracture in a composite plate. Part

I: Theory," J. Acoust. Soc. Am. **92**, 2964–2976 (1992).

[7] M. Bentahar and R. E. Gouerjuma, "Monitoring progressive damage in polymer based composite using nonlinear dynamics and acoustic emission," J. Acoust. Soc. Am., **125**, EL39–EL44 (2009).

[8] M. Ohtsu and Y. Tomoda, "Phenomenological model of corrosion process in reinforced concrete identified by acoustic emission," ACI Mater. J. **105**, 194–199 (2008).

[9] T. Shiotani, M. Ohtsu, and K. Ikeda, "Detection and evaluation of AE waves due to rock deformation," Constr. Build. Mater. **15**, 235–246 (2001).

[10] A. Anastassopoulos and T. P. Philippidis, "Clustering methodology for evaluation of acoustic emission from composites," J. Acoust. Emiss. **13**, 11–22 (1994).

[11] D. Soulioti, N. M. Barkoula, A. Paipetis, T. Matikas, T. Shiotani, and D. G. Aggelis, "Acoustic emission behaviour of steel fiber reinforced concrete under bending," Constr. Build. Mater. **23**, 3532–3536 (2009).

[12] T. Shiotani and D. G. Aggelis, "Evaluation of repair effect for deteriorated concrete piers of intake dam using AE activity," J. Acoust. Emiss. **25**, 69–79 (2007).